THE JOURNAL OF PHYSICAL CHEMISTRY B

ARTICLE

pubs.acs.org/JPCB

Effect of Solvent and Counterions upon Structure and NMR Spin−Spin Coupling Constants in Heparin Disaccharide

Miloš Hricovíni*

Institute of Chemistry, Slovak Academy of Sciences, 845 38 Bratislava, Slovakia

ABSTRACT: Density functional theory (DFT) has been used to analyze structure and NMR spin−spin coupling constants in heparin disaccharide. Both B3LYP/6-311++G** and M05−2X/6-311++G** methods have been used for optimization of disaccharide geometry. Solvent effect was treated by use of explicit water molecules. Solvent-caused variations of DFT-computed indirect one-bond proton−carbon coupling constants up to 17 Hz between isolated and solvated states, however, had a limited influence upon magnitudes of proton−proton spin−spin coupling constants. Interatomic distances and bond and torsion angles indicated that the structure of the 2-O-sulfated iduronic acid residue affected the geometry of the N,6-sulfated glucosamine residue. Optimized disaccharide geometry showed that the change of counterion (Ca^{2+} instead of Na^{+}) influenced geometry of pyranose rings and the glycosidic linkage conformation. DFT-computed three-bond proton−proton spin−spin coupling constants agreed well with published experimental data and indicated that the population of the $^{1}C_4$ chair form of the 2-O-sulfated iduronic acid residue increased in the presence of Ca^{2+} ions compared to the presence of Na^{+} ions. Analysis also showed that the Fermi contact term was not always dominant and that paramagnetic and diamagnetic contributions considerably influenced magnitudes of proton−proton spin−spin coupling constants.

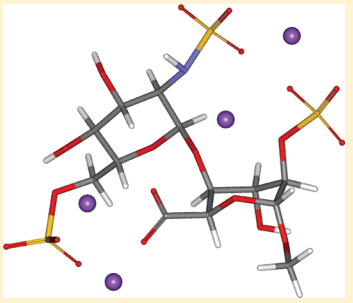

I. INTRODUCTION

Theoretical analyses of biologically active carbohydrates provide information on their 3D structures and are often used for interpretation of experimental data such as high-resolution NMR spin−spin coupling constants and nuclear Overhauser effects (NOEs). Density functional theory (DFT) methods are at present commonly used as they can yield reliable structures and energies of carbohydrate molecules in many cases at moderate computational costs.[1−6] However, despite advances in modeling of saccharide molecules, there are still difficulties associated with the influence of solvent upon molecular structure.[7−11] It is especially the case in substituted saccharides, such as glycosaminoglycans (GAGs), bearing sulfate and carboxylate groups. These molecules are considerably charged and, consequently, solvent together with counterions significantly affects their molecular structure and properties.

GAG molecules are constituted by disaccharide units of uronic acid and hexosamine and are involved in a number of important biological processes.[12−14] The most known and studied GAG molecule, heparin, is made up of uronic acid (iduronic acid and to a smaller extent glucuronic acid) and hexosamine, predominantly 2-amino-2-deoxy-D-glucose. These residues can be substituted by O- or N-sulfated (OSO_3^- or NSO_3^-) groups. Thus, heparin is a heterogeneous polymer mostly consisting of 2-O-sulfated iduronic acid residues (IdoA2S) and N,6-sulfated glucosamine residues (GlcN,6S). Ring conformations of IdoA2S residues have been the subject of particular interest.[15,16] NMR[15−19] and theoretical analyses[16,20−27] showed that this residue is flexible in heparin-like oligosaccharides, and three forms−namely $^{1}C_4$, $^{4}C_1$, and $^{2}S_0$−can contribute to the conformational equilibrium. The populations of these conformers depend upon the structure of neighboring units and type of counterions.[18,28]

Previous DFT calculations, by the B3LYP/6-311++G** method, yielded geometries and NMR parameters in structurally related compounds in isolated state or in solvent.[25,29] However, treatment of solvent applying reaction field methods[30] showed that these methods may not give reliable results for GAG molecules.[25] An explicit solvent model is physically more justified for charged molecules having strong interactions between solute and solvent.[7,8] In the present paper, data from quantum mechanical/molecular mechanical (QM/MM) calculations of heparin disaccharide are reported. The geometries were optimized by both B3LYP/6-311++G**/UFF and M05-2X/6-311++G**/UFF with explicit water molecules for two forms of heparin disaccharide differing in conformation ($^{1}C_4$ and $^{2}S_0$) of the IdoA2S residue. In order to validate the computed data, DFT-based NMR indirect spin−spin coupling constants were compared with published experimental values.

II. METHODS

The geometry of heparin disaccharide [methyl *O*-(2-deoxy-2-sulfamino-6-*O*-sulfo-α-D-glucopyranosyl)-(1→4)-2-*O*-sulfo-α-L-idopyranoside uronate tetrasodium salt; GlcN,6S-IdoA2S-OMe] molecule has been optimized with Gaussian03 and Gaussian09.[31] Density functional theory (DFT) was performed at the B3LYP[32] or M05-2X[33] level of theory. All geometry optimization was

Received: August 5, 2010
Revised: December 22, 2010
Published: January 21, 2011

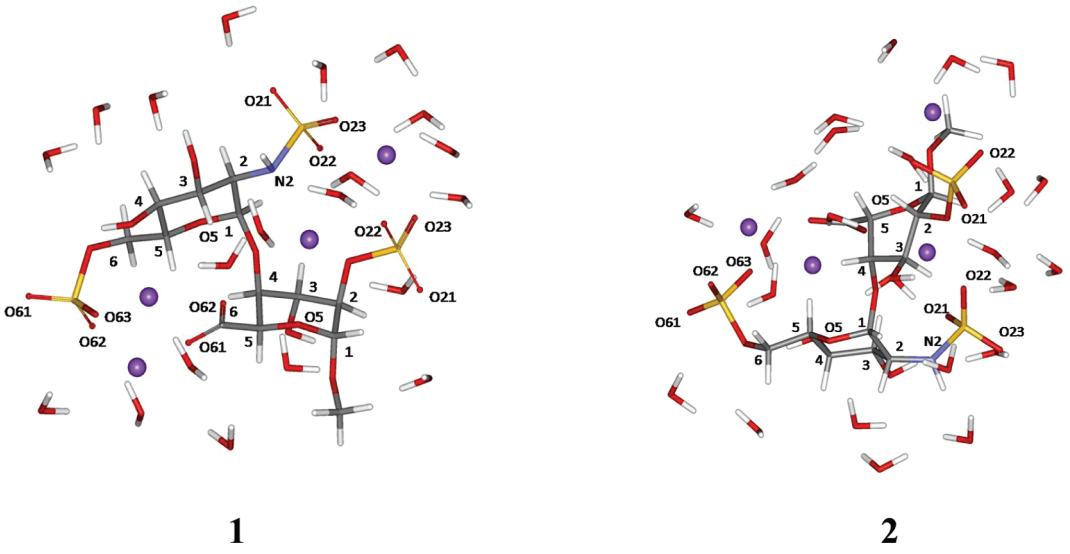

1 **2**

Figure 1. Structures of heparin disaccharide. Two forms **1** (left) and **2** (right) correspond to different conformations ($^1C_4$ and $^2S_0$) of the IdoA2S residue. The GlcN,6S residue is in the $^4C_1$ form. Violet dots represent sodium ions. Part of the water molecules is not shown in the picture for clarity.

performed with a 6-311++G** basis set. Hydration of disaccharide molecules was performed by explicit water molecules. The initial water positions were chosen on the basis of published crystal data of structurally related molecules.[34] Solvent was then treated within ONIOM approach by use of the UFF force field.[35] The IdoA2S residue was considered in two conformations ($^1C_4$ and $^2S_0$, Figure 1) whereas the GlcN,6S residue was in the $^4C_1$ conformation regardless of the IdoA2S form. NMR proton−proton and proton−carbon spin−spin coupling constants were computed at the B3LYP level. Averaged coupling constants were obtained by fitting of coupling constants for individual conformers to experimental values.

III. RESULTS AND DISCUSSION

A. Geometry. Selected optimized interatomic distances and bond and torsion angles in **1** and **2** (Figure 1) are listed in Tables 1−3. Bond lengths (Table 1) vary with the iduronate ring form and counterions not only in the IdoA2S residue but also in the GlcN,6S residue. The largest differences within the IdoA2S residue are in the S(2)−O and C6−O distances. Variations in both S(2)−O and C6−O separations are due to the presence of counterions in different positions with respect to oxygen atoms. For example, interatomic distances in the 2-O-sulfate group reveal that both S2−O21 and S2−O22 bonds are longer (1.499 and 1.491 Å) than the S2−O23 distance (1.446 Å) in the $^2S_0$ conformer in the presence of sodium ions. The bond lengths suggest the resonance bond character of the S2−O21 and S2−O22 linkages (both are involved in coordination with Na^+), whereas the S2−O23 bond has double bond character with the shorter separation. Even larger differences in bond lengths between the S═O double bond [$d_{S(N)-O23}$ = 1.456 Å] and the other two bonds [$d_{S(N)-O21}$ = 1.514 Å and $d_{S(N)-O22}$ = 1.493 Å] were obtained in the NSO_3^- group. The bond distance variations were analogous also in the 6-O-sulfate group, and similar trends were seen in the $^1C_4$ chair form of the IdoA2S. The above evidence of the two longer S−O bonds and one double bond in both NSO_3^- and OSO_3^- groups is in agreement with the published crystallographic data where the S−O distance of the double bond was 1.446 Å.[34] Na^+ ions are 6-fold coordinated with oxygens from sulfates and water molecules. Distances between sulfate oxygens and sodium atoms vary in a relatively small interval (2.25−2.66 Å), somewhat longer are water oxygens···sodium distances (2.89−3.62 Å) (Figure 2). Obviously, positions of Na^+ ions are different in **1** and **2** due to their structural differences. In the $^1C_4$ chair form (Figure 2A), the NSO_3^- group and the 2-OSO_3^- group on one side coordinate two sodium atoms, and similarly, the 6-OSO_3^- group and the COO^- group on the other side coordinate two sodium atoms (Figure 1). On the other hand, one Na^+ ion is coordinated with oxygens from the 2-OSO_3^- group and the anomeric oxygen from OMe in the skew form (Figure 2B).

Coordinations of divalent Ca^{2+} cations are also different in the $^1C_4$ chair form of the IdoA2S residue compared to the skew form. In the $^1C_4$ chair form, one calcium ion has coordination with six oxygens: ring oxygen (the IdoA2S residue), one from the 2-OSO_3^- group, glycosidic oxygen, one from the carboxylate group, one from the NSO_3^- group, and one water molecule. Further ligation is with nitrogen from the NSO_3^- group. Thus the Ca^{2+} cation has pentagonal bipyramidal ligation (Figure 3A). Four oxygens from the disaccharide (except for the ring oxygen) and the nitrogen form the base of the pentagonal bipyramid. The remaining two oxygens (ring oxygen from the IdoA2S residue and water) are below and above the plane. A second Ca^{2+} ion is coordinated with two oxygens from the 6-OSO_3^- group, carboxylate oxygen, OH(4), and three water molecules. In the skew form, the first Ca^{2+} cation is coordinated in a different way compared to the chair form (Figure 3B): the ion is ligated with two oxygens from the NSO_3^- group, one carboxylate, ring and glycosidic oxygens, together with two water molecules. Oxygen from the 2-OSO_3^- group and the nitrogen from the NSO_3^- group are not involved in interaction with calcium ion. The second calcium ion, has comparable coordination as in **1**. Thus, there is a tendency of Ca^{2+} ion to form pentagonal bipyramid-type coordination.

Variations in bond angles (Table 2) were most significant in the pendant groups; for example, the bond angles C2−N2−S-(N) (GlcN,6S) and C2−O2−S2 (IdoA2S) varied up to 14°. Within the pyranose rings, the largest changes were obtained in

dx.doi.org/10.1021/jp1098552 |J. Phys. Chem. B 2011, 115, 1503–1511

Table 1. Selected Optimized (B3LYP) Interatomic Distances in Heparin Disaccharide in the Presence of Na^+ and Ca^{2+} Ions[a]

	interatomic distance (Å)			
	Na^+		Ca^{2+}	
bond	$^1C_4$	$^2S_0$	$^1C_4$	$^2S_0$
	Residue IdoA2S			
C1−C2	1.540	1.536	1.529	1.548
C2−C3	1.547	1.537	1.528	1.538
C3−C4	1.548	1.540	1.538	1.536
C4−C5	1.539	1.542	1.535	1.541
C5−O5	1.435	1.439	1.426	1.440
C1−O5	1.436	1.439	1.436	1.438
C1−O1	1.395	1.430	1.420	1.356
C5−C6	1.531	1.537	1.532	1.527
S2−O2	1.706	1.697	1.702	1.784
S2−O21	1.500	1.499	1.504	1.478
S2−O22	1.481	1.491	1.443	1.456
S2−O23	1.463	1.446	1.462	1.468
C6−O61	1.281	1.257	1.276	1.246
C6−O62	1.249	1.258	1.240	1.288
H1−H2	2.581	3.050	2.555	3.004
H2−H3	2.580	3.057	2.550	3.059
H3−H4	2.582	2.975	2.493	2.989
H4−H5	2.456	2.385	2.453	2.445
H2−H5	3.854	2.320	4.055	2.454
	Residue GlcN,6S			
C1−C2	1.542	1.533	1.550	1.537
C2−C3	1.538	1.548	1.526	1.546
C3−C4	1.527	1.525	1.513	1.523
C4−C5	1.544	1.549	1.550	1.546
C5−O5	1.434	1.427	1.418	1.422
C1−O5	1.414	1.417	1.404	1.418
C1−O1	1.425	1.424	1.444	1.436
C5−C6	1.534	1.530	1.532	1.536
C2−N2	1.476	1.465	1.469	1.467
S(N)−N2	1.762	1.715	1.776	1.682
S(N)−O21	1.496	1.514	1.492	1.506
S(N)−O22	1.494	1.493	1.464	1.444
S(N)−O23	1.471	1.456	1.456	1.533
C6−O6	1.445	1.447	1.404	1.448
O6−S6	1.680	1.665	1.654	1.668
S6−O61	1.453	1.444	1.436	1.505
S6−O62	1.512	1.511	1.502	1.437
S6−O63	1.495	1.490	1.496	1.512
H1−H2	2.439	2.495	2.328	2.499
H2−H4	2.647	2.598	2.660	2.767
H3−H5	2.733	2.781	2.619	2.924

[a] Two conformers ($^1C_4$ and $^2S_0$) of the IdoA2S residue are considered. The GlcN,6S residue is in the $^4C_1$ form.

the anomeric part (e.g., O5−C1−O1, O5−C1−C2) in both residues. Coordination with different counterions resulted in noticeable differences in bond angles. This includes not only

Table 2. Selected Optimized (B3LYP) Bond Angles in Heparin Disaccharide in the Presence of Na^+ and Ca^{2+} Ions[a]

	angle (deg)			
	Na^+		Ca^{2+}	
bond angle	$^1C_4$	$^2S_0$	$^1C_4$	$^2S_0$
	Residue IdoA2S			
O5−C1−C2	109.5	111.9	109.6	108.7
O5−C1−O1	113.2	109.4	110.7	107.6
C5−O5−C1	111.8	113.9	112.9	108.4
C1−C2−C3	113.9	109.3	110.5	111.7
C2−O2−S2	122.0	120.1	115.8	116.9
	Residue GlcN,6S			
O5−C1−C2	109.6	109.0	110.2	107.5
O5−C1−O1	113.1	111.2	113.8	110.9
C5−O5−C1	116.6	114.1	118.9	114.8
C1−C2−C3	110.8	108.8	112.8	108.9
C1−O1−$C4_{IdoA}$	120.0	118.3	123.3	116.1
C2−N2−S(N)	112.9	126.0	113.1	126.1
C6−O6−S(6)	120.4	120.0	117.1	120.3

[a] Two conformers ($^1C_4$ and $^2S_0$) of the IdoA2S residue are considered. The GlcN,6S residue is in the $^4C_1$ form.

C2−O2−S2 (IdoA2S) angles (changed about 6° in the chair form) but glycosidic linkages bond angles ($C1_{GlcN,6S}$−O1−$C4_{IdoA2S}$) as well.

Values of torsion angles (Table 3) indicated that sulfate and carboxylate groups influenced ring geometries of both pyranose rings and pendant groups in the molecule. Apart from obvious differences in IdoA2S residues in **1** and **2**, there were also variations in the GlcN,6S residue. This comprises not only heavy atoms (e.g., variations in the torsion angle in the array O5−C1−C2−C3) but hydrogens as well. The differences, up to 20° (H1−C2−C3−H2, Ca^{2+}), are relatively large and result in different magnitudes of three-bond proton−proton coupling constants in the two disaccharide forms. Such an influence of the IdoA2S residue ring form upon the 3D structure of the GlcN,6S unit is remarkable. Effects of sulfate and carboxylate groups, counterions, and hydrogen bonds result in structural changes of pyranose ring forms of both residues. Furthermore, ϕ and ψ torsion angles (H1−C1−O1−$C4_{IdoA2S}$, H4−C4−O1−$C1_{GlcN,6S}$) at the glycosidic linkage also varied with the IdoA2S ring form.

Variations in overall molecular structures originate also from the effect of ions. Replacing sodium by calcium resulted in 40° difference of the ϕ torsion angle, whereas the ψ torsion angle changed nearly 20° in the $^1C_4$ chair form. Torsion angles among ring protons also varied mainly in the IdoA2S residue in the $^2S_0$ form. For example, the torsion angles between H1−H2 were 157° (Na^+ form) and 144° (Ca^{2+} form). Such variations in geometry affected also the magnitudes of proton−proton coupling constants (see later discussion). Furthermore, as sulfate groups are directly involved in interactions with counterions, their orientation was also influenced by the type of counterion. Previous analysis indicated that calcium and sodium exhibited different ways of binding: calcium bound specifically, whereas sodium showed territorial binding in heparin-like di- and hexasaccharides.[36−38] Presented data found differences in the form of binding between disaccharide and Na^+ compared to

dx.doi.org/10.1021/jp1098552 |J. Phys. Chem. B 2011, 115, 1503–1511

Table 3. Selected Optimized (B3LYP) Torsion Angles in Heparin Disaccharide in the Presence of Na^+ and Ca^{2+} Ions[a]

	angle (deg)			
	Na^+		Ca^{2+}	
torsion angle	$^1C_4$	$^2S_0$	$^1C_4$	$^2S_0$
Residue IdoA2S				
O5−C1−C2−C3	−48	30	−55	20
C6−C5−O5−C1	169	168	176	157
O5−C1−O1−C_{Me}	−74	−68	−74	−92
C1−C2−C3−C4	41	−61	49	−56
C2−C3−C4−C5	−44	24	−49	24
H1−C1−O5−C5	−179	148	−174	164
H5−C1−O5−C1	49	50	57	39
H1−C1−C2−C3	−163	−82	−172	−94
H3−C3−C2−C1	162	57	168	62
H1−C1−C2−H2	73	157	67	144
H2−C2−C3−H3	−75	179	−71	−177
H3−C3−C4−H4	77	143	71	143
H4−C4−C5−H5	56	40	51	46
H4−C4−O1−$C1_{Glc}$	−38	−49	−20	−44
Residue GlcN,6S				
O5−C1−C2−C3	56	63	49	65
C6−C5−O5−C1	177	176	177	176
O5−C1−O1−$C4_{IdoA}$	49	81	8	70
C1−C2−C3−C4	−54	−56	−52	−53
C2−C3−C4−C5	49	47	52	40
H1−C1−O5−C5	−177	177	−169	175
H5−C1−O5−C1	−66	−67	−66	−69
H1−C1−C2−C3	173	180	165	−179
H3−C3−C2−C1	65	61	68	63
H1−C1−O1−$C4_{IdoA}$	−68	−36	−108	−47
H1−C1−C2−H2	55	65	47	67
H2−C2−C3−H3	−179	174	−177	176
H3−C3−C4−H4	168	166	167	156
H4−C4−C5−H5	−166	−163	−168	−155

[a] Two conformers ($^1C_4$ and $^2S_0$) of the IdoA2S residue are considered. The GlcN,6S residue is in the $^4C_1$ form.

disaccharide and Ca^{2+}. Each of these ions bound specifically to negatively charged groups in the disaccharide: sodium had 6-fold coordination with oxygens (Figure 2), whereas calcium showed a tendency to form pentagonal bipyramidal coordination (Figure 3). There was at least one water molecule involved in coordination with Ca^{2+} or Na^+. However, no differences in the number of water molecules in coordination with these two different ions were observed. Comparison of the binding mechanism with ions presented in this work with the published data indicate that positions of Na^+ and Ca^{2+} ions in disaccharide fall within the most favorable regions found in previous molecular dynamic simulations for structurally related disaccharide and hexasaccharides.[37,38]

Comparison of the present data with those obtained in isolated state[29] indicated that solvent had relatively minor effects upon molecular geometry. Interatomic distances and bond angles were found to be comparable, while somewhat larger differences between isolated and solvated states were found in torsion angle magnitudes (up to 10° for H−C−C−H arrays of bonded atoms). It is interesting to note that even glycosidic linkage geometry has not been strongly influenced (1° for both ϕ and ψ torsion angles in the $^1C_4$ chair form). The largest difference was obtained for the H1−C1−O1−$C4_{IdoA}$ angle (−36° in water; −50° in vacuum)[29] in the $^2S_0$ form and resulted in different magnitudes of coupling constants (see later discussion). Comparison of presented torsion angles at the glycosidic linkage with those in polysaccharide heparin for the GlcN,6S−IdoA2S linkage (ϕ = −39° and ψ = −33° in the $^1C_4$ chair form; ϕ = −9° and ψ = −41° in the $^2S_0$ form)[14] indicates that ϕ values differ in disaccharide with respect to polysaccharide heparin whereas ψ angles are comparable in both molecules. The mentioned differences in ϕ angles are not surprising as conformational properties of disaccharides, compared to polysaccharides, can be quite different. There are major differences in steric effects and electrostatic interactions between these two types of molecules. The absence of large charged sulfates and carboxylates on neighboring units are particularly important factors that substantially affect 3D molecular structures in heparin disaccharides compared to polysaccharide heparin.

B. NMR Spin−Spin Coupling Constants. Computed three-bond proton−proton coupling constants ($^3J_{H-C-C-H}$) in heparin disaccharide are listed in Table 4. Data are presented for molecular geometries obtained by geometry optimization by both B3LYP (Na^+ and Ca^{2+} ions) and M05-2X (Na^+ ions) functionals for comparison. Inspection of the data indicates that interproton torsion angles in the GlcN,6S residue in **1** are very similar to each other regardless of the optimization method, whereas some differences are seen in the IdoA2S residue. As a result, $^3J_{H-C-C-H}$ magnitudes are smaller in this case for the B3LYP geometry than for the geometry obtained with the M05-2X functional. Larger differences between B3LYP and M05-2X geometries were found in the IdoA2S residue in **2**. For example, the H1−H2 torsion angle difference was 13° and the corresponding $^3J_{H-C-C-H}$ values were 7.03 Hz (B3LYP) and 5.14 Hz (M05-2X). Apart from that, the GlcN,6S residue geometry varied depending on conformation of the IdoA2S residue as well. Variations of torsion angles were up to 19° (H2−C2−C3−H3; M05-2X), and consequently the $^3J_{H-C-C-H}$ magnitudes changed considerably in some cases. $^3J_{H1,H2}$ were 3.79 Hz (**1**) and 1.93 Hz (**2**), respectively, for the M05-2X geometry. Similar large coupling constants differences in the GlcN,6S residues (9.25 and 7.55 Hz) were obtained also for $^3J_{H4,H5}$. Smaller but still significant discrepancies in $^3J_{H-C-C-H}$ values were found for the geometry optimized with the B3LYP functional.

As calcium ions are bivalent, disaccharide molecular geometry variations between Na^+ and Ca^{2+} ions are consequently bigger. Comparison of the data presented in Table 4 reveal that $^3J_{H-C-C-H}$ magnitudes in the presence of Na^+ ions differ significantly compared to those in the presence of Ca^{2+} ions in **1** and **2**. In the IdoA2S residue, $^3J_{H3,H4}$ values showed the largest difference (2.68 Hz for Na^+ and 4.35 Hz for Ca^{2+}) in **1**, together with the $^3J_{H1,H2}$ values (7.03 Hz for Na^+ and 4.42 for Ca^{2+}) in **2**. It should be noted that the differences in torsion angles for these proton pairs (77° for Na^+ vs 71° for Ca^{2+} for H3−H4 in **1** and 157° for Na^+ vs 144° for Ca^{2+} for H1−H2 in **2**) would not suggest such a significant difference in $^3J_{H-C-C-H}$ magnitudes. Thus other influences, such as different spin polarizations of electrons at these protons in the presence of bivalent calcium, play an important role in the mechanism of indirect proton−proton coupling constants (see later discussion). Differences in geometry, and consequently in $^3J_{H-C-C-H}$ values, are also pronounced

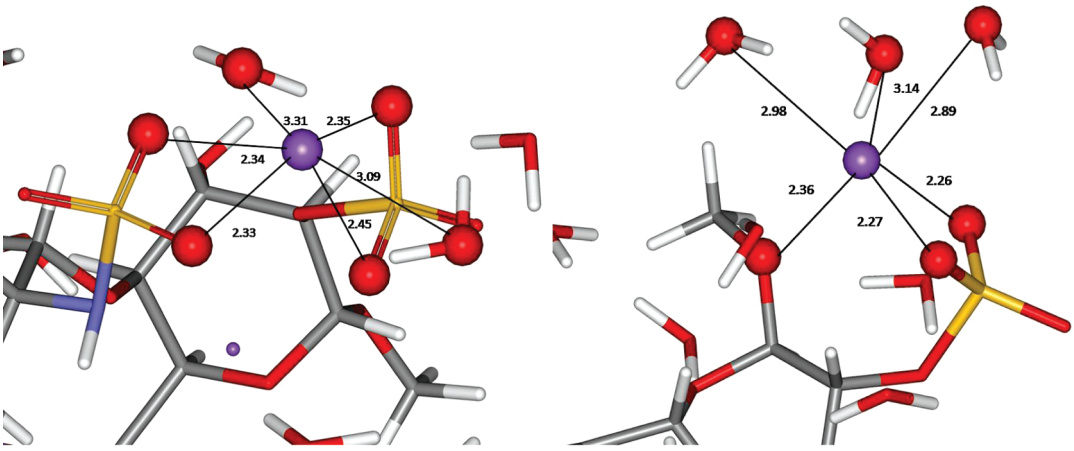

Figure 2. Interatomic distances (in angstroms) among oxygen atoms, belonging to disaccharide or solvent, and sodium ions. Oxygen atoms (red) involved in coordination with sodium ion (violet) are displayed as spheres. IdoA2S residues are either in the $^1C_4$ chair form (A) or the $^2S_0$ form (B).

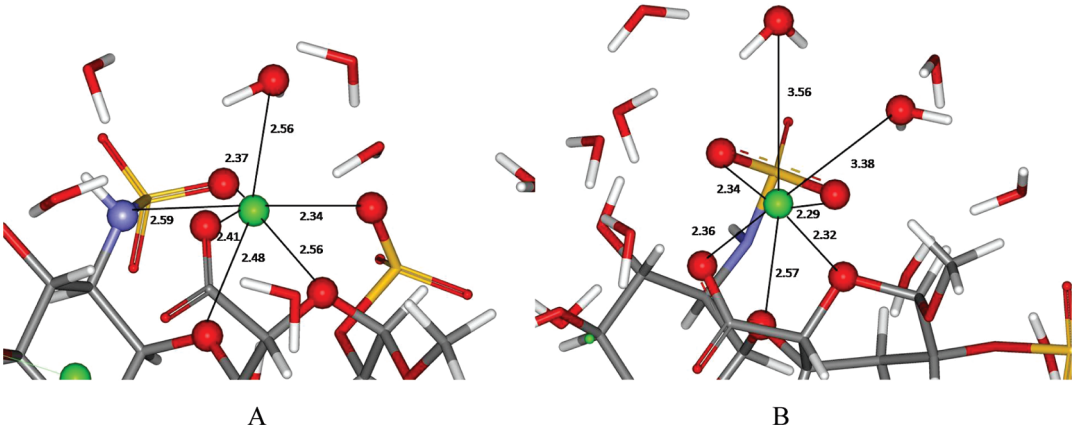

Figure 3. Interatomic distances (in angstroms) among oxygen atoms belonging to disaccharide or solvent, and calcium ions. Oxygen atoms (red) involved in coordination with calcium ion (green) are displayed as spheres. IdoA2S residues are either in the $^1C_4$ chair form (A) or in the $^2S_0$ form (B).

within the GlcN,6S residues in **1** and **2**. $^3J_{H1,H2}$ values (4.71 Hz in **1** and 2.44 Hz in **2**) in the GlcN,6S residues are good examples of differences in molecular geometries in **1** and **2** (torsion angles 47° and 67°, respectively) in the presence of Ca^{2+} ions. Experimentally, molecular geometry variations in the GlcN,6S residues have not been observed until recently as the measured scalar coupling constants are averaged and thus cannot reveal such geometry variations. Theoretically, such variations have already been discussed,[29] and recent analysis of residual dipolar couplings in heparin-like oligosaccharide[39] supported theoretical predictions.

Data also points out on complex mechanisms that affect $^3J_{H-C-C-H}$ magnitudes. Some coupling constants are considerably different from each other though they have comparable torsion angles. $^3J_{H1,H2}$ (1.49 Hz) and $^3J_{H3,H4}$ (2.68 Hz) in the IdoA2S residue ($^1C_4$ conformation; B3LYP geometry, Na^+) are more than 1 Hz different, but torsion angles among corresponding protons are nearly the same (73° vs 77°). The same is valid for $^3J_{H4,H5}$ (2.48 Hz) in the IdoA2S residue and $^3J_{H1,H2}$ (3.77 Hz) in the GlcN,6S residue (corresponding angles are 56° and 55°, respectively; B3LYP geometry, Na^+, structure **1**). As already mentioned, variations in coupling constants magnitudes for comparable torsion angles were seen also in the presence of Ca^{2+} ions.

An insight into these differences can be seen from Fermi contact (FC), paramagnetic spin−orbit (PSO), diamagnetic spin−orbit (DSO), and spin-dipolar (SD) contributions to coupling constants (Table 5). The Fermi term is 0.98 Hz in the $^3J_{H1,H2}$ and it is considerably smaller than in the $^3J_{H3,H4}$ coupling constant (2.26 Hz) in the IdoA2S residue in **1** (the difference in torsion angles for these two pairs of protons is 4°) pointing out on quite different polarization of the *s*-type electrons at various protons. Small FC contributions to overall magnitudes are quite evident for $^3J_{H-4,H-5}$ (1.63 and 3.36 Hz) in the IdoA2S residue in both **1** and **2**. On the other hand, the DSO (2.03 and 2.24 Hz, respectively) and PSO terms are comparable, or even bigger, than that of the FC in $^3J_{H-4,H-5}$. Consequently their overall contributions to total magnitude of coupling constants are significant even though the DSO and PSO contributions partially cancel each other due to their opposite signs.

Different polarization of C−H bonds and thus differences in the s-character of individual bonds is quite clear for H1−H2 and H4−H5 in IdoA2S in **1** as well as for H1−H2 in GlcN6S. The strong anisotropy of electron densities was seen mainly at C4−H4 and C5−H5 bonds in the IdoA2S residues in both **1** and **2**. Spin polarization of s-type electrons is most pronounced in the

dx.doi.org/10.1021/jp1098552 |*J. Phys. Chem. B* 2011, 115, 1503–1511

Table 4. Computed Three-Bond Proton−Proton Coupling Constants and Torsion Angles in Heparin Disaccharide in the Presence of Na^+ and Ca^{2+} Ions[a]

	Na^+		Na^+		Ca^{2+}	
array of atoms	torsion angle (deg), B3LYP	$^3J_{H-C-C-H}$ (Hz)	torsion angle (deg), M05-2X	$^3J_{H-C-C-H}$ (Hz)	torsion angle (deg), B3LYP	$^3J_{H-C-C-H}$ (Hz)
			Form **1**, Conformation $^1C_4$ of Residue IdoA2S			
H1−H2	73	1.49	67	2.02	67	1.96
H2−H3	−75	2.46	−69	3.45	−71	3.23
H3−H4	77	2.68	73	3.44	71	4.35
H4−H5	56	2.48	53	2.66	51	2.60
			Form **1**, Conformation $^4C_1$ of Residue GlcN,6S			
H1−H2	55	3.77	56	3.79	47	4.71
H2−H3	−179	11.43	−178	11.34	−177	11.88
H3−H4	168	9.27	170	9.32	167	9.55
H4−H5	−166	9.32	−168	9.25	−168	10.17
			Form **2**, Conformation $^2S_0$ of Residue IdoA2S			
H1−H2	157	7.03	144	5.14	144	4.42
H2−H3	179	11.22	−179	11.32	−177	11.23
H3−H4	143	3.75	147	4.75	143	4.12
H4−H5	40	4.33	38	4.89	46	3.63
			Form **2**, Conformation $^4C_1$ of Residue GlcN,6S			
H1−H2	65	2.68	71	1.93	67	2.44
H2−H3	174	11.34	163	11.21	176	12.50
H3−H4	166	9.17	173	10.03	156	8.26
H4−H5	−163	9.18	−154	7.55	−155	9.26

[a] Geometry was optimized by both B3LYP and M05-2X for Na^+ ions and by B3LYP for Ca^{2+} ions. Two forms (**1** and **2**) correspond to different conformations ($^1C_4$ and $^2S_0$) of the IdoA2S residue. The GlcN,6S residue is in the $^4C_1$ form.

above bonds leading to small magnitudes of the FC term in $^3J_{H4,H5}$. PSO contributions are also affected by electron densities; however, *p*-type polarization functions play a significant role in this case. The PSO term is the biggest also in $^3J_{H4,H5}$ in the IdoA2S residues and, together with small FC terms, leads to a decreased magnitude of these couplings. Though these effects are partially compensated by larger DSO values, the overall $^3J_{H4,H5}$ magnitudes remain small, which is in very good agreement with experiments. The same observations have been made previously in monosaccharide IdoA2S-OMe[25] and this disaccharide analyzed in isolated state.[29] In fact, calculations of magnitudes of coupling constants in heparin oligosaccharides using not properly parametrized relationships for $^3J_{H-C-C-H}$ upon torsion angles could not lead to satisfactory results and led to their higher values in many cases.

Other influences on $^3J_{H-C-C-H}$ magnitudes originate from solvent effects. Comparison of the $^3J_{H-C-C-H}$ magnitudes in isolated and solvated states in heparin disaccharide indicates that solvent plays a role in $^3J_{H-C-C-H}$ values. As mentioned, differences were found in the geometry of **2**, where torsion angles differed in some cases up to 10°. Consequently, computed coupling constants differed; however, due to the overall small magnitudes of proton−proton coupling constants, variations of their magnitudes were quite limited. The largest difference was found for $^3J_{H1,H2}$ in the IdoA2S residue in **2**. In general, bigger differences in proton−proton coupling constants were in most cases due to the choice of functional (M05-2X compared to B3LYP) rather than to the solvent effects. Variations between isolated and solvated states were found to be much more pronounced in the case for one-bond proton−carbon coupling constants ($^1J_{H-C}$) and three-bond proton−carbon coupling constants ($^3J_{H-C-C-C}$ and $^3J_{H-C-O-C}$). The biggest difference was 17 Hz in $^1J_{H1,C1}$ in the GlcN6S residue, reflecting mainly variations in the C1−H1 bond lengths. $^1J_{H-C}$ values for ring protons and carbons changed less, typically in the interval of 1−3 Hz (data not presented, manuscript in preparation). The role of solvent, analyzed in other biomolecules, also pointed out on effects upon coupling constant magnitudes. However, the overall differences between isotropic coupling constants in isolated and solvated states were not very pronounced.[8]

Averaged theoretical $^3J_{H-C-C-H}$ values in heparin disaccharide in the presence of Na^+ ions in solution, together with published data in the isolated state,[29] and experimental[40] values are shown in Table 6. Theoretical values (B3LYP geometry) obtained with the ratio $^1C_4$:$^2S_0$ = 80:20 are in very good agreement with experiments. The largest differences were obtained for $^3J_{H4,H5}$ in the GlcN,6S residue, similarly to isolated state. Theoretical values were likely affected by other factors (C4−C5 bond lengths, charges, O5 lone pairs) than torsion angles exclusively, as already discussed in this and previous papers.[25,29] However, considerable improvement was obtained in the $^3J_{H4,H5}$ in the IdoA2S residue, where this coupling decreased from 3.2 Hz (vacuum) to 2.8 Hz (explicit solvent), and it is much closer to the experimental value (2.6 Hz). In general, coupling constants based on the M05-2X geometry showed worse agreement with experimental data than those obtained by B3LYP geometry.

Table 5. Computed Fermi Contact, Spin-Dipolar, and Para- and Diamagnetic Spin−Orbit Contributions to the Three-Bond Proton−Proton Coupling Constants in 1 and 2[a]

	contribution to coupling constant (Hz)				
array of atoms	FC	SD	PSO	DSO	total $^3J_{H-C-C-H}$ (Hz)
Form **1**, Conformation $^1C_4$ of Residue IdoA2S					
H1−H2	0.98	0.05	−0.61	1.07	1.49
H2−H3	2.08	0.05	−0.58	0.91	2.46
H3−H4	2.26	0.05	−0.77	1.14	2.68
H4−H5	1.63	0.10	−1.28	2.03	2.48
Form **1**, Conformation $^4C_1$ of Residue GlcN,6S					
H1−H2	2.56	0.11	−1.23	2.03	3.77
H2−H3	11.79	0.04	0.72	−1.14	11.43
H3−H4	9.78	0.04	0.80	−1.35	9.27
H4−H5	9.67	0.03	0.66	−1.04	9.32
Form **2**, Conformation $^2S_0$ of Residue IdoA2S					
H1−H2	7.38	0.04	0.78	−1.17	7.03
H2−H3	11.58	0.05	0.69	−1.10	11.22
H3−H4	4.06	0.02	0.50	−0.83	3.75
H4−H5	3.36	0.15	−1.42	2.24	4.33
Form **2**, Conformation $^4C_1$ of Residue GlcN,6S					
H1−H2	2.18	0.08	−0.82	1.24	2.68
H2−H3	11.73	0.04	0.71	−1.14	11.34
H3−H4	9.60	0.04	0.74	−1.22	9.17
H4−H5	9.50	0.03	0.68	−1.05	9.18

[a] Data are based on B3LYP geometry of heparin disaccharide in the presence of Na^+ ions. FC, Fermi contact; SD, spin-dipolar; PSO, paramagnetic spin−orbit; DSO, diamagnetic spin−orbit

Table 6. Experimental and Computed Averaged Best-Fit Three-Bond Proton−proton Coupling Constants in Heparin Disaccharide in the Presence of Na^+ Ions

	$^3J_{H-C-C-H}$ (Hz)			
array of atoms	experimental[a]	computed, vacuum, 79:21[b]	computed, water, 80:20, B3LYP[c]	computed, water, 80:20, M05-2X[c]
Residue IdoA2S				
H1−H2	2.3	2.4	2.6	2.7
H2−H3	4.6	4.4	4.3	5.0
H3−H4	3.4	3.1	3.0	3.7
H4−H5	2.6	3.2	2.8	3.1
Residue GlcN,6S				
H1−H2	3.6	3.4	3.6	3.4
H2−H3	11.4	11.3	11.4	11.3
H3−H4	9.5	9.5	9.3	9.5
H4−H5	10.4	8.9	9.3	9.0

[a] Reference 40. [b] Reference 29. [c] This work.

Presented data thus showed that explicit solvent correctly described the structure of heparin disaccharide where DFT-computed coupling constants agreed very well with experiment. On the other hand, simple dielectric continuum models may not give structures that agree with experimental data having the skewed form as the most stable in structurally similar molecules.[41] Inappropriateness of the application of such a model has already been discussed in a previous study of monosaccharide IdoA2S-OMe.[25] NMR experimental data agreed with the existence of the $^1C_4$ chair form exclusively, whereas application of the continuum solvent model favored the $^2S_0$ form.

Table 7. Experimental and Computed Averaged Best-Fit Three-Bond Proton−Proton Coupling Constants in Heparin Disaccharide in the Presence of Ca^{2+} ions

	$^3J_{H-C-C-H}$ (Hz)	
array of atoms	experimental[a]	computed, water, 90:10
Residue IdoA2S		
H1−H2	2.9	2.2
H2−H3	3.5	4.0
H3−H4	3.2	4.3
H4−H5	2.6	2.7
Residue GlcN,6S		
H1−H2		4.0
H2−H3		11.9
H3−H4	9.5	9.4
H4−H5	9.0	10.0

[a] Reference 36.

Averaged theoretical $^3J_{H-C-C-H}$ and experimental values in the presence of Ca^{2+} ions are presented in Table 7. As known from NMR experiments, the presence of calcium ions, instead of sodium ions, causes higher population of the $^1C_4$ form.[28,36] Presented theoretical coupling constants correctly interpreted this trend and the best agreement of averaged $^3J_{H-C-C-H}$ values with experimental data[28,36] was obtained for the ratio $^1C_4$:$^2S_0$ ∼ 90:10. Compared with Na^+ counterions, time-averaged $^3J_{H4,H5}$ in the GlcN,6S residue was bigger than that experimentally determined. There are also bigger differences in $^3J_{H-C-C-H}$ values for the IdoA2S residue compared to the presented data for Na^+ ions. In this case, effects of divalent ion coordination could lead to greater pyranose ring geometry distorsions and consequently to higher deviations of proton−proton coupling constants.

Selected $^3J_{H-C-C-C}$ and $^3J_{H-C-O-C}$ values are listed in Table 8. Both types of coupling constants strongly depend upon torsion angles; however, the influences of stereoelectronic effects are considerable in this type of coupling constants as well. For example, magnitudes of $^3J_{H1,C1,O5,C5}$ in compound **1** are 7.39 Hz (IdoA2S in the $^1C_4$ form) and 6.43 Hz in the GlcN,6S residues, although torsion angles are comparable (−177° vs 177°, thus the same torsion angle assuming symmetric Karplus-type relationship at 180°). Different C1−O5 bond lengths, C1−O5−C5 bond angles, and spin polarization contributed to the above differences in $^3J_{H-C-O-C}$ magnitudes. $^3J_{H-C-C-C}$ magnitudes depended upon stereoelectronic effects noticeably less. Replacement of oxygen by carbon in the array H−C−C−C in $^3J_{H-C-C-C}$ resulted in smaller variations of magnitudes of coupling constants. The influence of oxygen electronegativity and the electron pairs has clear consequences in $^3J_{H-C-O-C}$ values. $^3J_{H-C-C-C}$ and $^3J_{H-C-O-C}$ values in **1** and **2** in the presence of Ca^{2+} are presented in Table 8. As mentioned, calcium had an appreciable effect upon the molecular geometry and $^3J_{H-C-O-C}$ changed considerably also in the GlcN,6S residues (e.g., $^3J_{H1,C1,C2,C3}$).

Table 8. Computed Three-Bond Proton−Carbon Coupling Constants in Heparin Disaccharide in the Presence of Na^+ and Ca^{2+} Ions (B3LYP Geometry)[a]

	$^3J_{H-C-X-C}$ (Hz)		
array of atoms	Na^+, water	Ca^{2+}, water	Na^+, vacuum[b]
Form **1**, Conformation $^1C_4$ of Residue IdoA2S			
H1−C1−O5−C5	5.45	4.73	4.40
H5−C1−O5−C1	2.51	1.65	2.27
H1−C1−C2−C3	3.11	3.34	2.35
H3−C3−C2−C1	3.93	4.31	3.07
H4−C4−O1−$C1_{Glc}$	3.23	4.21	3.17
Form **1**, Conformation $^4C_1$ of Residue GlcN,6S			
H1−C1−O5−C5	7.39	8.89	6.41
H5−C1−O5−C1	1.36	1.31	1.28
H1−C1−C2−C3	4.28	5.01	3.44
H3−C3−C2−C1	1.36	1.31	1.16
H1−C1−O1−$C4_{IdoA}$	0.68	0.76	0.81
Form **2**, Conformation $^2S_0$ of Residue IdoA2S			
H1−C1−O5−C5	5.61	4.63	5.17
H5−C1−O5−C1	2.76	3.04	3.37
H1−C1−C2−C3	0.56	0.03	0.01
H3−C3−C2−C1	1.81	1.66	1.30
H4−C4−O1−$C1_{Glc}$	3.33	3.06	3.30
Form **2**, Conformation $^4C_1$ of Residue GlcN,6S			
H1−C1−O5−C5	6.43	6.31	5.88
H5−C1−O5−C1	1.55	1.54	0.74
H1−C1−C2−C3	3.71	3.87	2.25
H3−C3−C2−C1	1.15	1.21	2.08
H1−C1−O1−$C4_{IdoA}$	3.54	2.13	1.97

[a] Two forms (**1** and **2**) correspond to different conformations ($^1C_4$ and $^2S_0$) of the IdoA2S residue. The GlcN,6S residue is in the $^4C_1$ form. [b] Reference 29.

Interglycosidic $^3J_{H-C-O-C}$ coupling constants are important parameters used in determination of oligosaccharide conformations. Computed values indicated that $^3J_{H1,C1,O1,C4(IdoA)}$ considerably differed in **1** (0.68 Hz) and **2** (3.54 Hz) in the presence of Na^+ ions. The same trend, though not that pronounced, was seen with Ca^{2+} counterions (0.76 Hz in **1** vs 2.13 Hz in **2**). Calcium influenced also the ψ torsion angle due to different coordination in **1** and **2**: the $^3J_{H4,C4,O1,C1(Glc)}$ magnitudes changed from 4.21 Hz in **1** to 3.06 Hz in **2**. The data thus point out that the glycosidic linkage conformation changes in **1** and **2** due to different forms of the IdoA2S residue. Further analysis of interglycosidic $^3J_{H-C-O-C}$ coupling constants showed that solvent (compared to vacuum) affected mainly the ϕ torsion angle at the glycoside linkage. The largest difference (3.54 Hz compared to 1.97 Hz) was observed in $^3J_{H1,C1,O1,C4(IdoA)}$ in **2**. ψ values, and consequently $^3J_{H4,C4,O1,C1(Glc)}$ values, were found to be comparable in vacuum and in solution.

IV. CONCLUSIONS

DFT calculations at the B3LYP/6-311++G** level of theory with explicit solvent molecules have been performed on complexes of heparin disaccharide with Na^+ and Ca^{2+} ions. Comparison of computed molecular geometries in **1** and **2** with data obtained in the isolated state indicated that solvent had a relatively minor effect upon overall molecular structure. Interatomic distances and bond angles were found to be comparable; somewhat larger discrepancies in torsion angles were found between isolated and solvated states (up to 10° for H−C−C−H arrays of bonded atoms). Glycosidic linkage geometry has been negligibly influenced in **1** (1° for both ϕ and ψ torsion angles). The largest difference (14°) was obtained for the H1−C1−O1−$C4_{IdoA}$ angle in **2**. However, more pronounced geometry variations were obtained due to the type of functionals used and suggested that the semiempirical hybrid functional B3LYP gives better geometry than the empirical M05-2X functional in this type of molecule.

Interatomic distances in sulfate groups showed the resonance bond character of two S−O bonds with longer separations (∼1.5 Å) and an S−O bond having double -bond character with the shorter separation (∼1.45 Å). Data also indicate that Na^+ ions are 6-fold coordinated with oxygens from sulfates and water molecules. Distances between sulfate oxygens and sodium atoms vary in a relatively small interval (∼2.2−2.7 Å), longer are water oxygen ···sodium distances (∼2.9−3.6 Å). Coordination of divalent Ca^{2+} cation showed pentagonal bipyramidal ligation. In such arrangement, four oxygens from disaccharide and the nitrogen formed the base of the pentagonal bipyramid. The analysis of molecular geometry also showed that conformation of the IdoA2S residue influenced the geometry of the GlcN,6S residue. This effect could be seen not only for the anomeric part of the GlcN,6S residue but also for torsion angles among protons, indicating flattering of the pyranose ring due to the skew form of the neighboring residue.

It was shown that replacement of Ca^{2+} instead of Na^+ had considerable effect upon the overall conformation in **1**. It is due to the differences at the glycosidic torsion angles, which differ 40° for ϕ and 18° for ψ. Torsion angles among ring protons changed mainly in the IdoA2S residue in the $^2S_0$ form and consequently caused variation in proton−proton coupling constants.

DFT-computed $^3J_{H-C-C-H}$ magnitudes, based on B3LYP or M05-2X geometries, differed from each other where the major variations were obtained in **2**. Analysis showed that the Fermi term was smaller than the PSO contributions to $^3J_{H-C-C-H}$ values in several cases. Quite different polarization of the s-type electrons at various protons then resulted in different $^3J_{H-C-C-H}$ magnitudes at comparable torsion angles. Computed averaged $^3J_{H-C-C-H}$ magnitudes in the IdoA2S residue, based on the conformer ratio $^1C_4$:$^2S_0$ = 80:20, agreed well with experimental values in aqueous solution. For Na^+ ions, coupling constants computed from the B3LYP disaccharide geometry matched better with experimental $^3J_{H-C-C-H}$ than those from the disaccharide geometry optimized with the M05-2X functional.

Further differences in disaccharide structure and NMR parameters were due to different counterions. Comparison of the data revealed that $^3J_{H-C-C-H}$ magnitudes in the presence of Ca^{2+} ions differ significantly compared to those in the presence of Na^+ ions in **1** and **2**. The variations were more than 2.5 Hz in some cases and confirmed experimental findings that calcium appreciably influences geometry and NMR parameters in heparin-like compounds. It should also be noted that, apart from torsion angles influences upon $^3J_{H-C-C-H}$ magnitudes, other influences, such as different spin polarizations of electrons at these protons in the presence of bivalent calcium, play an important role in the mechanism of indirect proton−proton coupling constants. $^3J_{H-C-C-H}$ values in the IdoA2S residue showed agreement

with experiments when the $^1C_4$ conformation was nearly exclusively populated (about 90%). The shift in favor of the chair conformer in the presence of calcium ions is agreement with the published experimental data.

Solvent effects were significant mainly for $^1J_{H-C}$ values and partially for interglycosidic $^3J_{H-C-O-C}$ coupling constants. Averaged $^3J_{H-C-C-H}$ magnitudes were not significantly affected by solvent molecules. Computed interglycosidic $^3J_{H-C-O-C}$ coupling constants indicated that $^3J_{H1,C1,O1,C4(IdoA)}$ differ considerably (nearly 3 Hz) in **1** and **2** in the presence of Na^+ ions. The same trend, though not that pronounced, was seen with Ca^{2+} counterions. However, calcium also influenced the ψ torsion angle due to different coordination in **1** and **2**, where the difference in $^3J_{H4,C4,O1,C1(Glc)}$ was more than 1 Hz. The data thus point out at the glycosidic linkage conformation changes in **1** and **2** due to different forms of the IdoA2S residue in heparin disaccharide.

AUTHOR INFORMATION

Corresponding Author

*Tel +421-2-59410323; fax +421-2-59410222; e-mail hricovini@savba.sk.

ACKNOWLEDGMENT

This research was supported by VEGA Grant 2/0108/08.

REFERENCES

(1) Cloran, F.; Carmichael, I.; Serianni, A. S. *J. Phys. Chem. A* **1999**, *103*, 3783–3795.
(2) Tvaroška, I.; Taravel, F. R.; Utille, J. P.; Carver, J. P. *Carbohydr. Res.* **2002**, *337*, 353–367.
(3) Momany, F. A.; Appel, M.; Willett, J. L.; Schnupf, U.; Bosma, W. B. *Carbohydr. Res.* **2006**, *341*, 525–537.
(4) Czonka, G. I.; French, A. D.; Johnson, G. P.; Storz, C. A. *J. Chem. Theory Comput.* **2009**, *5*, 679–692.
(5) Karamat, S.; Fabian, W. M. F. *J. Phys. Chem. A* **2008**, *112*, 1823–1831.
(6) Hricovíni, M.; Malkina, O. L.; Bízik, F.; Turi-Nagy, L.; Malkin, V. G. *J. Phys. Chem. A* **1997**, *101*, 9756–9762.
(7) Pecul, M.; Ruud, K. *Magn. Reson. Chem.* **2004**, *42*, S128–S137.
(8) Sychrovský, V.; Schneider, B.; Hobza, P.; Žídek, L.; Sklenár, V. *Phys. Chem. Chem. Phys.* **2003**, *5*, 734–739.
(9) Sawada, T.; Fedorov, D. G.; Kitaura, K. *Int. J. Quantum Chem.* **2009**, *109*, 2033–2045.
(10) Aidas, K.; Mogelhoj, A.; Kjar, H.; Nielsen, C. B.; Mikkelsen, K. V.; Ruud, K.; Christiansen, O.; Kongsted, J. *J. Phys. Chem. A* **2007**, *111*, 4199–4210.
(11) Prabhakar, R.; Vreven, T.; Frisch, M. J.; Morokuma, K.; Musaev, D. G. *J. Phys. Chem. B* **2006**, *110*, 13608–13613.
(12) Conrad, H. E. *Heparin-Binding Proteins*; Academic Press: San Diego, CA, 1998.
(13) Casu, B.; Lindahl, U. *Adv. Carbohydr. Chem. Biochem.* **2001**, *57*, 159–208.
(14) Mulloy, B.; Forster, M. J.; Jones, C.; Davies, D. B. *Biochem. J.* **1993**, *293*, 849–858.
(15) Torri, G.; Casu, B.; Gatti, G.; Petitou, M.; Choay, J.; Jacquinet, J. C.; Sinay, P. *Biochem. Biophys. Res. Commun.* **1985**, *128*, 134–140.
(16) Ferro, D. R.; Provasoli, A.; Ragazzi, M.; Torri, G.; Casu, B.; Gatti, G.; Jacquinet, J. C.; Sinay, P.; Petitou, M.; Choay, J. *J. Am. Chem. Soc.* **1986**, *108*, 6773–6778.
(17) Hricovíni, M.; Nieto, P. M.; Torri, G. *NMR Spectroscopy of Glycoconjugates*; Jimenez-Barbero, J., Peters, P., Eds.; Wiley−VCH: Weinheim, Germany, 2002; pp 189−229.
(18) Ferro, D. R.; Provasoli, A.; Ragazzi, M.; Casu, B.; Torri, G.; Bossennec, V.; Perly, B.; Sinay, P.; Petitou, M.; Choay, J. *Carbohydr. Res.* **1990**, *195*, 157–167.
(19) Mikhailov, D.; Linhardt, R. J.; Mayo, K. H. *Biochem. J.* **1997**, *328*, 51–61.
(20) Ragazzi, M.; Ferro, D. R.; Provasoli, A. *J. Comput. Chem.* **1986**, *7*, 105–112.
(21) Forster, M. J.; Mulloy, B. *Biopolymers* **1993**, *33*, 575–588.
(22) Angulo, J.; Nieto, P. M.; Martin-Lomas, A. *Chem. Commun.* **2003**, *13*, 1512–1513.
(23) Ernst, S.; Venkataraman, G.; Sasisekharan, V.; Langer, R.; Cooney, C. L.; Sasisekharan, R. *J. Am. Chem. Soc.* **1998**, *120*, 2099–2107.
(24) Kurihara, Y.; Ueda, K. *Carbohydr. Res.* **2006**, *341*, 2565–2574.
(25) Hricovíni, M. *Carbohydr. Res.* **2006**, *341*, 2575–2580.
(26) Tissot, B.; Salpin, J. Y.; Martinez, M.; Gaigeot, M. P.; Daniel, R. *Carbohydr. Res.* **2006**, *341*, 598–609.
(27) Pol-Fachin, L.; Verli, H. *Carbohydr. Res.* **2008**, *343*, 1435–1445.
(28) Rabenstein, D. L.; Robert, J. M.; Peng, J. *Carbohydr. Res.* **1995**, *278*, 239–256.
(29) Hricovíni, M.; Scholtzová, E.; Bízik, F. *Carbohydr. Res.* **2007**, *342*, 1350–1356.
(30) Leach, A. R. *Molecular Modelling. Principles and Applications*; Prentice Hall: New York, 2001.
(31) Frisch, M. J.; Trucks, G. W.; Schlegel, H. B.; Scuseria, G. E.; Robb, M. A.; Cheeseman, J. R.; Montgomery, J. A., Jr.; Vreven, T.; Kudin, K. N.; Burant, J. C.; Millam, J. M.; Iyengar, S. S.; Tomasi, J.; Barone, V.; Mennucci, B.; Cossi, M.; Scalmani, G.; Rega, N.; Petersson, G. A.; Nakatsuji, H.; Hada, M.; Ehara, M.; Toyota, K.; Fukuda, R.; Hasegawa, J.; Ishida, M.; Nakajima, T.; Honda, Y.; Kitao, O.; Nakai, H.; Klene, M.; Li, X.; Knox, J. E.; Hratchian, H. P.; Cross, J. B.; Bakken, V.; Adamo, C.; Jaramillo, J.; Gomperts, R.; Stratmann, R. E.; Yazyev, O.; Austin, A. J.; Cammi, R.; Pomelli, C.; Ochterski, J. W.; Ayala, P. Y.; Morokuma, K.; Voth, G. A.; Salvador, P.; Dannenberg, J. J.; Zakrzewski, V. G.; Dapprich, S.; Daniels, A. D.; Strain, M. C.; Farkas, O.; Malick, D. K.; Rabuck, A. D.; Raghavachari, K.; Foresman, J. B.; Ortiz, J. V.; Cui, Q.; Baboul, A. G.; Clifford, S.; Cioslowski, J.; Stefanov, B. B.; Liu, G.; Liashenko, A.; Piskorz, P.; Komaromi, I.; Martin, R. L.; Fox, D. J.; Keith, T.; Al-Laham, M. A.; Peng, C. Y.; Nanayakkara, A.; Challacombe, M.; Gill, P. M. W.; Johnson, B.; Chen, W.; Wong, M. W.; Gonzalez, C.; Pople, J. A. *Gaussian 03*, revision C02; Gaussian, Inc., Wallingford, CT, 2004.
(32) Lee, C.; Yang, W.; Paar, R. G. *Phys. Rev. B.* **1988**, *37*, 785–789.
(33) Zhao, Y.; Schultz, N. E.; Truhlar, D. G. *J. Chem. Theory Comput.* **2006**, *2*, 364–382.
(34) Yates, E. A.; Mackie, W.; Lamba, D. *Int. J. Biol. Macromol.* **1995**, *17*, 219–223.
(35) Rappé, A. K.; Casewit, C. J.; Colwell, K. S.; Skiff, W. M. *J. Am. Chem. Soc.* **1992**, *114*, 10024–10035.
(36) Angulo, J.; Luis de Paz, J.; Nieto, P. M.; Martín-Lomas, M. *Isr. J. Chem.* **2000**, *40*, 289–299.
(37) Chevalier, F.; Angulo, J.; Lucas, R.; Nieto, P. M.; Martín-Lomas, M. *Eur. J. Org. Chem.* **2002**, 2367–2376.
(38) Chevalier, F.; Lucas, R.; Angulo, J.; Martín-Lomas, M.; Nieto, P. M. *Carbohydr. Res.* **2004**, *339*, 975–983.
(39) Jin, L.; Hricovíni, M.; Deakin, J. A.; Lyon, M.; Uhrín, D. *Glycobiology* **2009**, *19*, 1185–1196.
(40) LaFerla, B.; Lay, L.; Guerrini, M.; Poletti, L.; Panza, L.; Russo, G. *Tetrahedron* **1999**, *55*, 9867–9880.
(41) Remko, M.; von der Lieth, C. W. *J. Chem. Inf. Model.* **2006**, *46*, 1687–1694.